Structural consequences of hydrogen intercalation of epitaxial graphene on SiC(0001)

Jonathan D. Emery,[1,a)] Virginia H. Wheeler,[2] James E. Johns,[1] Martin E. McBriarty,[1] Blanka Detlefs,[3] Mark C. Hersam,[1] D. Kurt Gaskill,[2] and Michael J. Bedzyk[1,4,a)]
[1]*Department of Materials Science and Engineering, Northwestern University, Evanston, Illinois 60208, USA*
[2]*U.S. Naval Research Laboratory, Washington, DC 20375, USA*
[3]*ESRF—The European Synchrotron, CS 40220, 71, Avenue des Martyrs, 38043 Grenoble, France*
[4]*Department of Physics and Astronomy, Northwestern University, Evanston, Illinois 60208, USA*

(Received 10 September 2014; accepted 11 October 2014; published online 23 October 2014)

The intercalation of various atomic species, such as hydrogen, to the interface between epitaxial graphene (EG) and its SiC substrate is known to significantly influence the electronic properties of the graphene overlayers. Here, we use high-resolution X-ray reflectivity to investigate the structural consequences of the hydrogen intercalation process used in the formation of quasi-free-standing (QFS) EG/SiC(0001). We confirm that the interfacial layer is converted to a layer structurally indistinguishable from that of the overlying graphene layers. This newly formed graphene layer becomes decoupled from the SiC substrate and, along with the other graphene layers within the film, is vertically displaced by ~2.1 Å. The number of total carbon layers is conserved during the process, and we observe no other structural changes such as interlayer intercalation or expansion of the graphene *d*-spacing. These results clarify the under-determined structure of hydrogen intercalated QFS-EG/SiC(0001) and provide a precise model to inform further fundamental and practical understanding of the system. © *2014 AIP Publishing LLC*. [http://dx.doi.org/10.1063/1.4899142]

The unique properties of graphene hold great potential for use in nanoelectronics,[1–4] and one of the most practical routes for wafer-scale production of high-quality graphene is by the thermal decomposition of SiC to produce epitaxial graphene (EG).[5,6] EG/SiC exhibits the electronic and structural properties characteristic of graphene and remains the most promising form of graphene for use in state-of-the-art devices such as quantum resistance standards and radio frequency field-effect transistors.[7,8] In the case of epitaxial graphene on Si-terminated SiC [EG/SiC(0001)], however, the inferior electron mobility and increased charge carrier scattering[9–12] are often attributed to the influence of the ubiquitous $(6\sqrt{3}\times 6\sqrt{3})R30°$ (*6R3*) interfacial layer.[9,13–15] Recently, though, it has been demonstrated that high-temperature annealing of EG/SiC(0001) in H_2 leads to the intercalation of hydrogen to the interface.[16] In this process, the hydrogen breaks the Si–C bonds between the electronically inactive, but structurally graphene-like interface layer and the SiC(0001) (hereafter referred to as SiC) surface, thereby decoupling the interfacial layer from the substrate. The resultant "quasi-free-standing" (QFS) graphene exhibits enhanced carrier mobility and density, and field-effect transistors made from QFS-EG/SiC show higher current saturation and transconductance, and improved extrinsic current gain response.[17,18] Furthermore, these improved properties are accompanied by a reversal in dopant type from *n*- to *p*-type. This result emphasizes the considerable effect of the local environment on such low-dimensional electronic structures.

This resultant QFS-EG/SiC structure, in which it is believed that the newly decoupled graphene layer sits atop a H-saturated hexagonal SiC surface cell,[16,18] possesses an interfacial structure distinct from as-grown (AG) EG/SiC. The Si-H termination is thought to chemically and electronically passivate the terminal SiC layer, and the subsequent decoupling of the interfacial layer from the substrate eliminates much of its detrimental influence. Regardless, the electronic properties of QFS-EG/SiC generally remain markedly inferior as compared to those made from suspended graphene,[19] SiO_2-supported transferred graphene,[20] or EG grown on the carbon-terminated surface of SiC(000$\bar{1}$).[21] It therefore begs the question: What influence does the newly formed Si-H terminated SiC interface have on the overlying graphene? Only with precise understanding of the physical, chemical, and electronic structure of the interface can this question be addressed.

In this work, we investigate the atomic scale structure of H-intercalated QFS-EG/SiC using synchrotron-based high-resolution X-ray reflectivity (XRR). Our analysis reveals the positions of the constituent atomic layers along the SiC[0001] direction with sub-Å resolution and verifies the decoupling and vertical displacement of the C-only interfacial layer from the substrate after H intercalation. Previously, some structural properties of QFS-EG/SiC have been inferred using from core-level and angle-resolved X-ray photoelectron spectroscopy (XPS),[16] scanning tunneling microscopy (STM),[14] low-energy electron microscopy (LEEM),[16] and transmission electron microscopy (TEM).[22] However, these approaches are either destructive or largely incapable of accessing the buried interface structure with the sensitivity afforded by XRR. We also consider proposed alternative structural models, such as the possibility of hydrogen intercalation between graphene layers.

Two semi-insulating, nominally identical 0.4° offcut 6H-SiC substrates (II-VI, Inc.), cleaved from the same wafer,

[a)]Authors to whom Correspondence should be addressed. Electronic addresses: jdemery@anl.gov, Tel.: (630) 252-4665 and bedzyk@northwestern.edu, Tel.: (847) 491-3570.

Report Documentation Page

Form Approved
OMB No. 0704-0188

1. REPORT DATE	2. REPORT TYPE	3. DATES COVERED
23 OCT 2014		**00-00-2014 to 00-00-2014**

4. TITLE AND SUBTITLE	5a. CONTRACT NUMBER
Structural consequences of hydrogen intercalation of epitaxial graphene on SiC(0001)	5b. GRANT NUMBER
	5c. PROGRAM ELEMENT NUMBER
6. AUTHOR(S)	5d. PROJECT NUMBER
	5e. TASK NUMBER
	5f. WORK UNIT NUMBER
7. PERFORMING ORGANIZATION NAME(S) AND ADDRESS(ES) **Northwestern University,Department of Materials Science and Engineering,Evanston,IL,60208**	8. PERFORMING ORGANIZATION REPORT NUMBER
9. SPONSORING/MONITORING AGENCY NAME(S) AND ADDRESS(ES)	10. SPONSOR/MONITOR'S ACRONYM(S)
	11. SPONSOR/MONITOR'S REPORT NUMBER(S)

12. DISTRIBUTION/AVAILABILITY STATEMENT
Approved for public release; distribution unlimited

13. SUPPLEMENTARY NOTES

14. ABSTRACT

15. SUBJECT TERMS

16. SECURITY CLASSIFICATION OF:			17. LIMITATION OF ABSTRACT	18. NUMBER OF PAGES	19a. NAME OF RESPONSIBLE PERSON
a. REPORT **unclassified**	b. ABSTRACT **unclassified**	c. THIS PAGE **unclassified**	**Same as Report (SAR)**	**5**	

were first etched in 80 slm flowing H_2 at 1520 °C for 0.5 h in order to remove polishing damage. Samples were then graphitized under identical conditions (1540 °C in 100 mbar Ar for 0.42 h) in an Aixtron/Epigress VP508 Hot-Wall CVD reactor. Following graphitization, both samples were cooled to 1050 °C in Ar, at which point the pressure was increased to 900 millibar of either Ar- or Pd-purified H_2. Both samples were annealed for 0.5 h in these respective environments and then cooled to 700 °C before evacuating the chamber. Samples were removed from the reactor and exposed to ambient before cooling to room temperature. The in Ar- and H_2-annealed are hereafter referred to as as-grown AG-EG/SiC and QFS-EG/SiC, respectively. After transfer in ambient, samples were then loaded into UHV and degassed for 1 h at 500 °C for low-energy electron diffraction (LEED) measurements.

XRR measurements were performed under He flow at beamline 6-ID-B at the Advanced Photon Source (APS) at Argonne National Laboratory. Measurements were performed using = 15.00 keV (wavelength $\lambda = 0.8265$ Å) X-rays, following the methods described in Refs. 23 and 24. Data were fit between $q_z = 0.4$ to 6.6 $Å^{-1}$, where $q_z = 4\pi \mathrm{Sin}(2\theta/2)/\lambda$ is the out-of-plane component of the momentum transfer and 2θ is the scattering angle. Reflectivity is plotted as a function of 6H-SiC reciprocal lattice units (SiC r.l.u) $L = (c_{SiC}\ q_z)/2\pi$, where $c_{SiC} = 15.12$ Å is the 6H-SiC lattice parameter.

LEED patterns for control and H_2-processed EG/SiC [Figures 1(a) and 1(b)] verify the intercalation of the H to the interface as originally observed by Riedl *et al.*[16] Figure 1(a) shows the typical pattern for as-grown EG/SiC, exhibiting (*hk*) spots indexed to the SiC(10) and EG(10) reciprocal lattice rods, as well as the *6R3* superstructure spots associated with the interfacial layer. After annealing in H_2, the 6*R*3 spots are suppressed while the EG peaks increase in relative intensity [Fig. 1(b)]—a hallmark that the intercalation process has occurred.[16]

X-ray reflectivity data and best-fit models are shown in Fig. 2. The XRR data from the AG-EG/SiC sample is comparable to that observed in Ref. 13 and other similar works.[23,25] Comparatively, the QFS-EG/SiC shows orders-of-magnitude differences in scattered intensity at certain L values, signifying a distinct change in the interfacial structure. The most prominent of these differences are at $L \sim 5.5$ and $L \sim 12.5$, where the QFS-EG/SiC data show deep minima where none existed before H intercalation.

AG-EG/SiC and QFS-EG/SiC electron density (N_e) profiles derived from the fits in Fig. 2(a) are shown in Figs. 2(b) and 2(c), and corresponding interfacial ball-and-stick models are presented in Figs. 3(a) and 3(b). These profiles are calculated from models comprised of k atomic layers defined by their positions (z_k), occupancies (Θ_k), and distribution widths (σ_k), as described in Refs. 23 and 26, and normalized to the electron density of an ideal Si layer within the SiC substrate ($N_e/N_{Si} = 1$). We base this model on the results of our previous work, in which the interfacial structure of AG-EG/SiC was resolved using XRR in conjunction with X-ray standing wave-enhanced XPS.[13] Using this model, the data were fit with an interfacial layer comprised of two distinct C layers and a five-layer graphene film with monotonically reducing layer occupancy with increasing height above the SiC surface. However, this initial model yielded very poor fits, especially in the low-q_z region, resulting in goodness-of-fit χ^2 values[27] greater than 80. The source of this original poor fit is unclear, but the poor fits are limited to the low-q_z region, indicating the presence of nm-scale, near-surface electron density contrast. We therefore employed a model which included a jellium-like electron density distribution within the top few SiC bilayers. This model yields greatly improved XRR fit results, reducing the best-fit χ^2 value by over an order of magnitude to $\chi^2 = 5.27$ for AG-EG/SiC. The electron density profile in Fig. 2(b) corresponds to the best-fit AG-EG/SiC data in Fig. 2(a) and finds the interface layer to be, apart from the disordered component, statistically identical to that found in Ref. 13. Possible sources for this disorder may be small quantities of SiO_x inclusions or

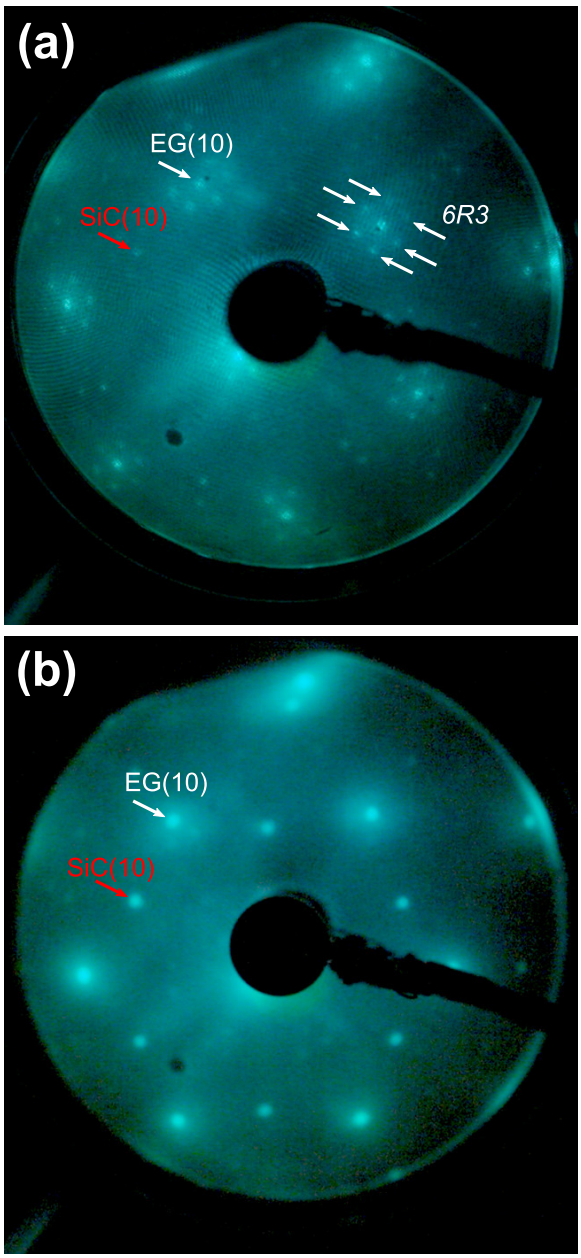

FIG. 1. LEED patterns at 130 eV for AG- and QFS-EG/SiC. SiC(10) and EG(10) LEED spots are indicated in red and white, respectively. (a) Before intercalation, the typical *6R3* superstructure spots are evident. (b) After intercalation, the *6R3* spots are strongly suppressed and the EG spots increase in relative intensity.

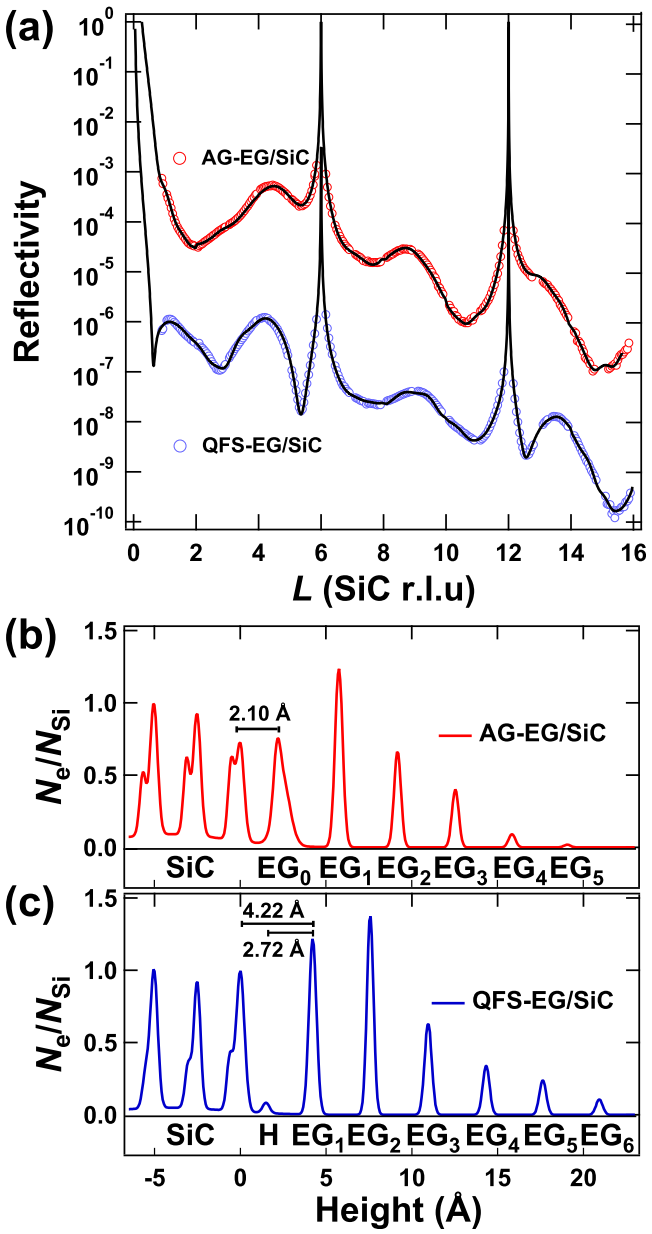

FIG. 2. XRR data and best fits, together with their corresponding electron density profiles, for AG- and QFS-EG/SiC. (a) AG-EG/SiC (red) and QFS-EG/SiC (blue) data are plotted with best-fit curves. Qualitatively, the two curves show sharp contrast, especially in the regions near $L \sim 5.5$ and ~ 12.5, indicating a distinct change in the interfacial structure upon H intercalation. (b) The electron density profile for AG-EG/SiC corresponding to the fit in (a). A broad interfacial layer (EG_0) is comprised of two distinct C distributions with an electron density maximum 2.1 Å above the terminal Si. (c) The QFS-EG/SiC electron density shows that the interfacial layer in (b) has been converted to a layer with graphene-like density positioned 4.22 Å above the SiC surface. Layer coverage and EG d-spacing are conserved upon H intercalation. For clarity, the AG-EG/SiC data and fits in (a) are offset vertically by a factor of 10^3.

remnant growth defects. Regardless, this component does not appear to affect fit results above the region of $L > 3$, and therefore we contend that the atomic-scale structural analysis is robust. AG-EG/SiC fitting results for the z_k, Θ_k, and σ_k parameters for the graphene ($k = 1$–5) and interfacial layers ($k = 0$) are reported in Table I.

The XRR result for AG-EG/SiC was used as the preliminary model for the analysis of the QFS-EG/SiC data. The best-fit result is shown in Fig. 2(a), and the associated

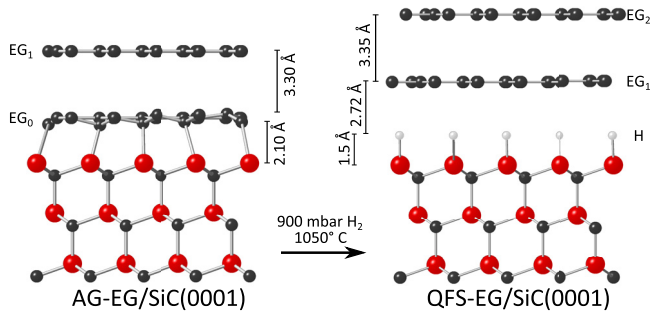

FIG. 3. Ball-and-stick representations of the conversion from AG-EG/SiC to QFS-EG/SiC as derived from XRR analysis in Figure 2. H, C, and Si atoms are colored in white, black, and red, respectively.

electron density profile is shown in Fig. 2(c). Best-fit results for z_k, Θ_k, and σ_k parameters for the graphene ($k = 1$–6) and H layer ($k = H$) are reported in Table I. Here, a H layer whose occupancy was constrained to that of the topmost Si layer was added at the nominal Si–H bond distance of 1.5 Å. Due to its low electron density, the fit results were largely insensitive to the structural details of the H monolayer (ML), although its inclusion did improve the best-fit χ^2 value by ~ 1. The total graphene coverage of the partially occupied layers for QFS-EG/SiC is 3.0 ML, which is ~ 1 EG ML greater than that of the AG-EG/SiC sister sample, as would be expected as the interfacial layer converts to an undistorted graphene layer. As observed by comparing Figs. 2(b) and 2(c), the EG_0 layer transforms into an EG_1 layer which is shifted upwards and sharpened. The characteristic ~ 1 Å corrugation of the interfacial layer[13,28] is reduced in amplitude, making the layer more graphene-like, as is consistent with STM studies.[14] Previous observations that S_1 and S_2 XPS components convert to EG components corroborate this result.[16] This newly formed EG_1 is displaced from the terminal Si in the SiC by 4.2 Å, or similarly, from the nominal H monolayer, by 2.7 Å. χ^2 mapping of the absolute position of the newly formed EG_1 layer indicates high confidence in this value within the limits of the model: 3-sigma confidence levels for the Si-EG_1

TABLE I. XRR-derived positions (z_k), atomic layer occupancies (Θ_k), and distribution widths (σ_k) for AG- and QFS-EG/SiC for each k layer in the model. z_k is reported with respect to the topmost Si in the SiC substrate and atomic Θ_k are reported normalized to an ideal EG/SiC monolayer; $\Theta = 1.00$ corresponds to 38.20 C/nm^2 (the areal density of C atoms in a graphene layer). Note that the areal density of Si within the SiC surface unit cell is 12.17 Si/nm^2; therefore, a saturated Si-H monolayer corresponds to a coverage of $\Theta = 0.32$ when reported normalized to an ideal EG/SiC monolayer. Starred values were held during fitting.

		AG-EG/SiC			QFS-EG/SiC		
k		z_k (Å)	Θ_k	σ_k (Å)	z_k (Å)	Θ_k	σ_k (Å)
H		…	…	…	1.5*	0.26*	0.1*
0	S_2	2.10	0.26	0.1	…	…	…
	S_1	2.45	0.73	0.40			
1		5.75	1.00	0.15	4.22	1.00	0.1
2		9.17	0.48	0.11	7.57	1.00	0.14
3		12.54	0.29	0.1*	10.95	0.50	0.09
4		15.84	0.06	0.1*	14.33	0.25	0.1*
5		19.07	0.01	0.1*	17.64	0.19	0.1*
6		…	…	…	20.93	0.08	0.1*

displacement are $4.22^{+0.06}_{-0.08}$ Å. In addition, the average interlayer spacing between the graphene sheets for the QFS-EG/SiC EG is 3.34 Å, which agrees closely with that of AG-EG/SiC (3.33 Å). This agreement verifies that the intercalation process has essentially no effect on the interplanar spacing of the EG film.

The $2.72^{+0.06}_{-0.08}$ H-EG_1 displacement compares to within 0.1 Å of recently calculated results using density functional theory.[29,30] Moreover, recent work by Rajput *et al.* has shown that the Dirac point of monolayer QFS-EG/SiC can shift by nearly 500 meV as the H-EG_1 separation is varied between 2.0 and 3.5 Å, inferring that the hole density may change by orders of magnitude as a result of subtle changes in interfacial displacement. The shift of the Dirac point defines the Schottky barrier height and will determine the practicality of employing the wide-bandgap semiconducting SiC substrate in a Schottky junction for application in, for example, graphene-based three-terminal vertical field-effect transistors.[31] The precise structural result presented herein is therefore useful in informing both computational and applied efforts in determining the electronic influence of the QFS-EG/SiC interface.

A final observation concerns the influence of H intercalation on the interlayer spacing of the graphene film itself. It remains an open question as to whether the high temperature processing of AG-EG/SiC in H_2 results in the intercalation of H species between the graphene sheets themselves in addition to decoupling the interfacial layer from the substrate. Laboratory-based X-ray diffraction and TEM results by Tokarczyk *et al.* suggest that the EG film may expand, with the observed *p*-type doping resulting from negatively charged H ions positioned between the graphene layers.[22] However, in their diffraction analysis, the authors do not account for the effect of the surface truncation and interfacial structure on the X-ray scattering profile, factors which we observe cause a shift in the absolute *L* position of the graphene film's (0002) peak by −0.2 SiC r.l.u (Fig. 2). While our data agree qualitatively with the observations of Tokarczyk *et al.*,[22] by accounting for the influence of the interfacial structure on the XRR intensity, we find the average interlayer graphene spacing for AG- and QFS-EG/SiC layers to be statistically identical. We emphasize that while XRR is not directly sensitive to the presence of hydrogen between the graphene sheets, H interlayer species are predicted to cause large average graphene interlayer expansion even for nanoscale graphene flakes (EG(0002) ∼3.7–3.9 Å)[32] or very low H/C concentrations (EG(0002) ∼4.4 Å).[33] Such EG interlayer expansion is not observed in this work despite the ∼0.1 Å confidence of the XRR model fits to the average graphene interlayer separation spacing. This suggests that if, indeed, the H intercalation process produces trapped interplanar H species, they do not modify the interplanar graphene spacing averaged over large (∼μm) lateral length scales.

In summary, we used X-ray reflectivity to compare the structures of two sister EG/SiC samples, one of which underwent H intercalation. Utilizing a previously established structural model for AG-EG/SiC,[13] we are able to verify the physical decoupling of the interfacial layer from the SiC substrate upon H-intercalation, its displacement along the SiC[0001] direction, and the conservation of the total coverage of overlayer carbon. We report, with 3-sigma confidence, the vertical displacement of the newly formed EG layer to be $4.22^{+0.06}_{-0.08}$ Å above the SiC terminus, or $2.72^{+0.06}_{-0.08}$ Å above the nominal H layer. Our structure is in close agreement with recent calculations[29] and has implications on the electronic behavior of the graphene overlayers themselves. This investigation of the structural consequences of H intercalation of EG/SiC precisely determines key physical parameters (e.g., SiC-EG displacement and interlayer graphene spacing) that are thought to critically influence technologically relevant properties such as Dirac point shift and Schottky barrier height. Furthermore, this methodology should prove valuable in the continued exploration of the myriad of atomic species that can be intercalated into EG/SiC interface (see Ref. 34 and references therein), many of which exhibit unique influence on the electronic properties of the overlying epitaxial graphene. Indeed, tailored interfacial design via intercalation may ultimately prove to be an important tool in the engineering of properties of epitaxial graphene on SiC. Similar studies on such analogous systems will prove critical to the development, understanding, and utilization in these promising new graphene systems.

We acknowledge support from MRSEC (NSF Grant No. DMR-1121262) and support from the Office of Naval Research. We acknowledge use of ID32 at the ESRF, as well as 5-ID-C and 6-ID-B at the APS, a DOE facility supported under Contract No. DE-AC02-06CH11357 to Argonne National Laboratory (ANL). This material is partially based upon work supported by the National Science Foundation Graduate Research Fellowship under Grant No. DGE-0824162. We acknowledge Sang-Soo Lee and Paul Fenter (ANL), as well as Jörg Zegenhagen (ESRF) for valuable discussions concerning this work. J.E.J. and M.C.H. acknowledge the Department of Energy (DE-FG02-09ER16109) and a W. M. Keck Foundation Science and Engineering Grant.

[1]C. Berger, Z. Song, T. Li, X. Li, A. Y. Ogbazghi, R. Feng, Z. Dai, A. N. Marchenkov, E. H. Conrad, P. N. First *et al.*, "Ultrathin epitaxial graphite: 2D electron gas properties and a route toward graphene-based nanoelectronics," J. Phys. Chem. B **108**(52), 19912–19916 (2004).
[2]C. Berger, Z. Song, X. Li, X. Wu, N. Brown, C. Naud, D. Mayou, T. Li, J. Hass, A. Marchenkov *et al.*, "Electronic confinement and coherence in patterned epitaxial graphene," Science **312**(5777), 1191–1196 (2006).
[3]Y.-M. Lin, C. Dimitrakopoulos, K. A. Jenkins, D. B. Farmer, H.-Y. Chiu, A. Grill, and P. Avouris, "100-GHz transistors from Wafer-scale epitaxial graphene," Science **327**(5966), 662 (2010).
[4]J. Baringhaus, M. Ruan, F. Edler, A. Tejeda, M. Sicot, A. T. Ibrahimi, Z. Jiang, E. H. Conrad, C. Berger, C. Tegenkamp *et al.*, "Exceptional ballistic transport in epitaxial graphene nanoribbons," Nature **506**(7488), 349–354 (2014).
[5]K. V. Emtsev, A. Bostwick, K. Horn, J. Jobst, G. L. Kellogg, L. Ley, J. L. McChesney, T. Ohta, S. A. Reshanov, J. Röhrl *et al.*, "Towards wafer-size graphene layers by atmospheric pressure graphitization of silicon carbide," Nat. Mater. **8**(3), 203–207 (2009).
[6]Y.-M. Lin, A. Valdes-Garcia, S.-J. Han, D. B. Farmer, I. Meric, Y. Sun, Y. Wu, C. Dimitrakopoulos, A. Grill, P. Avouris *et al.*, "Wafer-scale graphene integrated circuit," Science **332**(6035), 1294–1297 (2011).
[7]A. Tzalenchuk, S. Lara-Avila, A. Kalaboukhov, S. Paolillo, M. Syväjärvi, R. Yakimova, O. Kazakova, T. J. B. M. Janssen, V. Fal'Ko, and S. Kubatkin, "Towards a quantum resistance standard based on epitaxial graphene," Nat. Nanotechnol. **5**(3), 186–189 (2010).
[8]J. Moon, D. Curtis, M. Hu, D. Wong, C. McGuire, P. Campbell, G. Jernigan, J. L. Tedesco, B. VanMil, R. Myers-Ward *et al.*, "Epitaxial-

graphene RF field-effect transistors on Si-face 6H-SiC substrates," IEEE Electron Device Lett. **30**(6), 650–652 (2009).
[9]K. V. Emtsev, F. Speck, T. Seyller, L. Ley, and J. D. Riley, "Interaction, growth, and ordering of epitaxial graphene on SiC{0001} surfaces: A comparative photoelectron spectroscopy study," Phys. Rev. B **77**(15), 155303 (2008).
[10]J. Ristein, S. Mammadov, and T. Seyller, "Origin of doping in quasi-free-standing graphene on silicon carbide," Phys. Rev. Lett. **108**(24), 246104 (2012).
[11]N. Ray, S. Shallcross, S. Hensel, and O. Pankratov, "Buffer layer limited conductivity in epitaxial graphene on the Si face of SiC," Phys. Rev. B **86**(12), 125426 (2012).
[12]W. A. de Heer, C. Berger, M. Ruan, M. Sprinkle, X. B. Li, Y. K. Hu, B. Q. Zhang, J. Hankinson, and E. Conrad, "Large area and structured epitaxial graphene produced by confinement controlled sublimation of silicon carbide," Proc. Nat. Acad. Sci. USA **108**(41), 16900–16905 (2011).
[13]J. D. Emery, B. Detlefs, H. J. Karmel, L. O. Nyakiti, D. K. Gaskill, M. C. Hersam, J. Zegenhage, and M. J. Bedzyk, "Chemically resolved interface structure of epitaxial graphene on SiC(0001)," Phys. Rev. Lett. **111**(21), 215501 (2013).
[14]S. Goler, C. Coletti, V. Piazza, P. Pingue, F. Colangelo, V. Pellegrini, K. V. Emtsev, S. Forti, U. Starke, F. Beltram *et al.*, "Revealing the atomic structure of the buffer layer between SiC (0001) and epitaxial graphene," Carbon **51**, 249–254 (2012).
[15]S. Kim, J. Ihm, H. J. Choi, and Y.-W. Son, "Origin of anomalous electronic structures of epitaxial graphene on silicon carbide," Phys. Rev. Lett. **100**(17), 176802 (2008).
[16]C. Riedl, C. Coletti, T. Iwasaki, A. A. Zakharov, and U. Starke, "Quasi-free-standing epitaxial graphene on SiC obtained by hydrogen intercalation," Phys. Rev. Lett. **103**(24), 246804 (2009).
[17]J. A. Robinson, M. Hollander, M. LaBella III, K. A. Trumbull, R. Cavalero, and D. W. Snyder, "Epitaxial graphene transistors: enhancing performance via hydrogen intercalation," Nano Lett. **11**(9), 3875–3880 (2011).
[18]F. Speck, J. Jobst, F. Fromm, M. Ostler, D. Waldmann, M. Hundhausen, H. B. Weber, and T. Seyller, "The quasi-free-standing nature of graphene on H-saturated SiC (0001)," Appl. Phys. Lett. **99**(12), 122106 (2011).
[19]K. I. Bolotin, K. Sikes, Z. Jiang, M. Klima, G. Fudenberg, J. Hone, P. Kim, and H. L. Stormer, "Ultrahigh electron mobility in suspended graphene," Solid State Commun. **146**(9), 351–355 (2008).
[20]J.-H. Chen, C. Jang, S. Xiao, M. Ishigami, and M. S. Fuhrer, "Intrinsic and extrinsic performance limits of graphene devices on SiO2," Nat. Nanotechnol. **3**(4), 206–209 (2008).
[21]M. Orlita, C. Faugeras, P. Plochocka, P. Neugebauer, G. Martinez, D. K. Maude, A. L. Barra, M. Sprinkle, C. Berger, W. A. de Heer *et al.*, "Approaching the Dirac point in high-mobility multilayer epitaxial graphene," Phys. Rev. Lett. **101**(26), 267601 (2008).
[22]M. Tokarczyk, G. Kowalski, M. Możdżonek, J. Borysiuk, R. Stępniewski, W. Strupiński, P. Ciepielewski, and J. M. Baranowski, "Structural investigations of hydrogenated epitaxial graphene grown on 4H-SiC (0001)," Appl. Phys. Lett. **103**(24), 241915 (2013).
[23]J. D. Emery, Q. H. Wang, M. Zarrouati, P. Fenter, M. C. Hersam, and M. J. Bedzyk, "Structural analysis of PTCDA monolayers on epitaxial graphene with ultra-high vacuum scanning tunneling microscopy and high-resolution X-ray reflectivity," Surf. Sci. **605**(17–18), 1685–1693 (2011).
[24]P. Fenter, J. G. Catalano, C. Park, and Z. Zhang, "On the use of CCD area detectors for high-resolution specular X-ray reflectivity," J. Synchrotron Radiat. **13**, 293–303 (2006).
[25]J. Hass, J. Millán-Otoya, P. First, and E. Conrad, "Interface structure of epitaxial graphene grown on 4H-SiC (0001)," Phys. Rev. B **78**(20), 205424 (2008).
[26]I. Robinson and D. Tweet, "Surface x-ray diffraction," Rep. Prog. Phys. **55**(5), 599 (1992).
[27]$\chi^2 = (N-N_p)^{-1}\Sigma_k((I_{meas,k}-I_{calc,k})^2/Err_k^2)$, where $I_{meas,k}$ and $I_{calc,k}$ are the measured and calculated intensities of the k^{th} data point, respectively. Err_k is the uncertainty for the data point, and N and N_p represent the total number of data points and fitting parameters, respectively.
[28]F. Varchon, P. Mallet, J. Y. Veuillen, and L. Magaud, "Ripples in epitaxial graphene on the Si-terminated SiC(0001) surface," Phys. Rev. B **77**(23), 235412 (2008).
[29]A. Markevich, R. Jones, S. Öberg, M. Rayson, J. Goss, and P. Briddon, "First-principles study of hydrogen and fluorine intercalation into graphene-SiC (0001) interface," Phys. Rev. B **86**(4), 045453 (2012).
[30]S. Rajput, M. Chen, Y. Liu, Y. Li, M. Weinert, and L. Li, "Spatial fluctuations in barrier height at the graphene–silicon carbide Schottky junction," Nat. Commun. **4**, 2752 (2013).
[31]H. Yang, J. Heo, S. Park, H. J. Song, D. H. Seo, K.-E. Byun, P. Kim, I. Yoo, H.-J. Chung, and K. Kinam, "Graphene barristor, a triode device with a gate-controlled Schottky barrier," Science **336**(6085), 1140–1143 (2012).
[32]R. S. Aga, C. L. Fu, M. Krčmar, and J. R. Morris, "Theoretical investigation of the effect of graphite interlayer spacing on hydrogen absorption," Phys. Rev. B **76**(16), 165404 (2007).
[33]Y. Miyabe, T. Yoshida, S. Muto, T. Kiyobayashi, and H. Wasada, "Hydrogen trapping state associated with the low temperature thermal desorption spectroscopy peak in hydrogenated nanostructured graphite," J. Appl. Phys. **104**(4), 044311 (2008).
[34]U. Starke, S. Forti, K. Emtsev, and C. Coletti, "Engineering the electronic structure of epitaxial graphene by transfer doping and atomic intercalation," MRS Bull. **37**(12), 1177–1186 (2012).